

# Merging Uncertainty into Probabilistic Octree Models of 3-D Perturbed Workspaces

P. Payeur<sup>†</sup>, D. Laurendeau<sup>†</sup>, C. M. Gosselin<sup>‡</sup>

Computer Vision and Digital Systems Laboratory

<sup>†</sup> Dept of Electrical and Computer Engineering

<sup>‡</sup> Dept of Mechanical Engineering

Laval University

Sainte-Foy, Québec, Canada, G1K 7P4

<http://www.gel.ulaval.ca/~vision>

[ppayeur, laurend, gosselin]@gel.ulaval.ca

## Abstract

In a previous paper, a closed-form approximation of probability distribution which takes into account the sensor uncertainty has been presented to build probabilistic occupancy models of 3-D environments from range data. In this paper, the approach is extended in order to simultaneously consider the uncertainty on spatial relationships between various reference frames implied in autonomous data gathering. A data gathering strategy which allows compensation of external perturbations is presented. Uncertainty propagation methods for a chain of three spatial relationships in three dimensions are developed and compared. Finally, the closed-form approximation of probability distribution is extended to allow the uncertainty from all sources to be considered while building the model with respect to a generic reference frame.

## 1 Introduction

Modeling of a robot workspace based on data provided by sensors mounted on a moving vehicle or robot arm is an essential capability for an autonomous system to operate in complex environments. The necessity to maintain correlation between data gathered from various viewpoints is a critical issue in building reliable models required in many tasks such as planning collision-free paths for a mobile robot or a telemanipulator working in dangerous areas.

Correlation between measurements is difficult to maintain because of the uncertainty on the vehicle or arm displacement between each viewpoint from which data are gathered. Various sources of uncertainty may be involved. Sensor characteristics is one of the main sources, but there is also some uncertainty which results from the mechanical calibration of the components of the autonomous system. Moreover, external perturbations can induce noise on the measurements which must be quantified and compensated before merging these data into the model. Kalman filtering is a powerful tool to deal with such problems [3, 4] but uncertainty can also be processed independently from the measurements.

Since the uncertainty sources are distributed among the components of the modeling system, some means are needed to propagate the uncertainties from their respective reference frame to the global reference frame which supports the model. If the uncertainty originating from each source is propagated without deformation, it can be stored into the model and used as an additional criterion in the selection of the safer collision-free path.

Jacobian matrices computed from the geometrical relationships between the respective reference frames of the sensor, the vehicle or the arm, and the workspace model can be used to propagate the uncertainty. Smith *et al.* [12] have developed the equations to be used when the global transformation between the sensor and the model reference frames involves a composition of two primitive transformations which are both affected by some uncertainty. The resulting expressions are of average complexity. This complexity grows with the addition of other uncertain transformations. The evaluation of the covariance matrices when inverse transformations are involved also results in an increase of the complexity unless some approximation is used.

Julier and Uhlmann [5] proposed a probabilistic approach which can be used to propagate the uncertainty through nonlinear relationships such as those implied between each reference frame. The complexity of this approach also depends on the number of independent reference frames involved in the propagation but the estimation of covariance matrices is replaced by an intermediate probabilistic distribution which is less computationally intensive.

Both of these schemes can be envisioned in the application considered in this work. This application consists in building probabilistic occupancy grid models of a telemanipulator workspace in order to plan collision-free paths. The telerobotic system under development is intended to service on-line electricity distribution equipments. In previous papers [8, 9], an approach has been presented which allows to build probabilistic occupancy grids of a 3-D workspace in a computationally tractable manner. This strategy is based on a closed-form

approximation used to estimate the occupancy probability of space regions around each viewpoint. The closed-form approximation processes each range measurement and computes the occupancy probability along the laser beam line. Considering that the range sensor measurements are characterized by a Gaussian error distribution, the occupancy probability reaches a maximum value at the object surface while it is set to 0% (*empty*) between the sensor and the object and to 50% (*unknown*) behind the object. For each viewpoint the closed-form approximation is applied and the resulting occupancy probability distribution is temporarily stored into a local spherical occupancy grid. An algorithm which merges local occupancy probabilistic distributions (OPD) is then used to build a global Cartesian probabilistic octree model as shown in figure 1. In the original scheme, only the uncertainty originating from the range sensor is taken into account and the spatial relationships between each OPD reference frame is considered as error free. It is now intended to consider the uncertainty associated to each spatial transformation relating the local OPD to the model reference frame in order to encode this supplementary information into the probabilistic occupancy model.

In this paper, a data gathering strategy is presented in the context of the electricity distribution line maintenance task. Uncertainty propagation methods are detailed and compared in terms of complexity and suitability to the probabilistic model building approach in a 3-dimensional workspace. This approach is also extended such that the uncertainty originating from the sensor as well as from the spatial relationships can be taken into account in the workspace occupancy model.

Section 2 describes the data gathering strategy which allows to take into account the external perturbations on an outdoor scene. Section 3 details the exhaustive uncertainty propagation approach by means of Jacobian matrices and the development proposed by Smith *et al.* extended to a sequence of three successive spatial transformations.

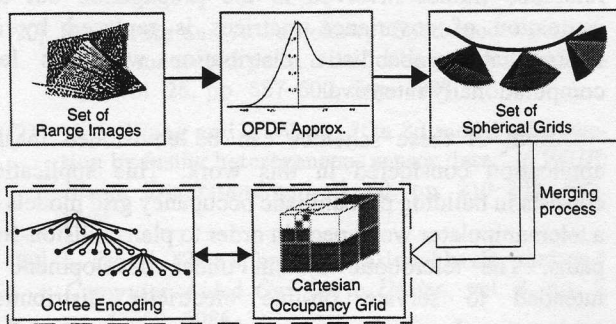


**Figure 1 :** Processing of range measurements by means of the closed-form OPD approximation and merge of local spherical occupancy grids.

Section 4 describes the Julier and Uhlmann strategy adapted to the 3-transformation composition as needed for the data gathering strategy. In section 5, the integration of uncertainty into the closed-form OPD approximation is presented in accordance with the occupancy probabilistic model building scheme. Finally, considerations about the overall complexity and the importance of uncertainty integration into occupancy models for collision-free path planning are presented in the context of power line maintenance applications.

## 2 Range data gathering on an outdoor scene submitted to perturbations

Any wide spread scene is submitted to external uncontrolled perturbations when located in an outdoor environment. Wind effect is of particular importance on an electrical pole assembly as shown in figure 2 since it produces oscillations both on the rigid structure and on the wires. To build an occupancy model in actual operating conditions when such perturbations occur, the relative motion between the sensor and the scene must be compensated. Otherwise, the model would be less reliable. In the power line maintenance application, sensors are located on a working platform at the extremity of a boom truck. Therefore, both the pole and the sensors are submitted to external perturbations.

One solution to deal with this problem consists in grabbing simultaneously range data from multiple viewpoints covering the whole region of interest [6]. This provides a stable model at the instant the measurements are taken but this model cannot be used to guide a robot since the scene and the boom continue to oscillate. Therefore, such a data gathering strategy provides models which are valid only instantaneously.

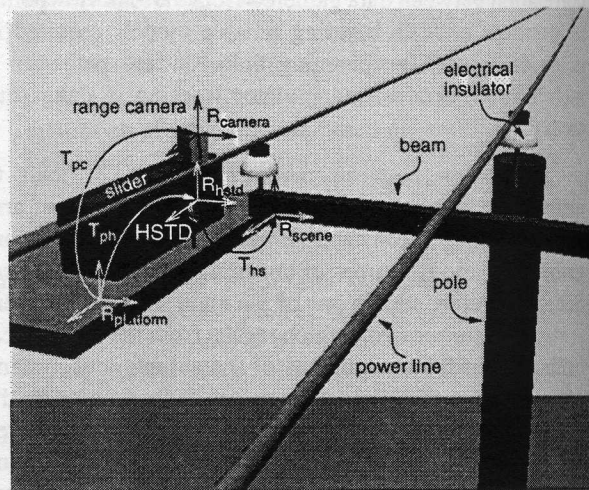


**Figure 2 :** Data gathering setup and related spatial relationships in the context of an electricity line maintenance application.

Another solution that has been tested and adopted integrates a single laser range sensor which can rotate and translate on a slider mounted on the working platform. While grabbing images, a dedicated sensor currently under development in our laboratory acts as a high speed tracking device (HSTD) to keep track of the relative position and orientation of the scene in respect to the working platform. The HSTD consists of a video camera with a laser beam mounted on a fast orienting device that tracks a reference point attached for instance to the extremity of the beam in the scene. The spatial relationship,  $T_{hs}$ , between the HSTD reference frame,  $R_{hstd}$ , and the scene reference frame,  $R_{scene}$ , is extracted from the image provided by the HSTD video camera. Given that the HSTD keeps tracking the scene during data gathering as well as while the telemanipulator interacts with the scene, a representative model can be computed and used during manipulation since external perturbations can be compensated.

A constraint to satisfy in order to obtain such a model is that the model is built in a reference frame attached to the scene,  $R_{scene}$ . Since this reference frame is submitted to the same perturbations as the pole, while  $R_{hstd}$  is submitted to perturbations affecting the boom, the knowledge of  $T_{hs}$  allows to close the transformation chain between the range camera reference frame,  $R_{camera}$ , and  $R_{scene}$  at any time. As seen in figure 2, the spatial relationships between the HSTD ( $R_{hstd}$ ), the platform ( $R_{platform}$ ) and the range camera ( $R_{camera}$ ) are obtained by means of mechanical calibration. These are fixed parameters except for  $T_{pc}$  which is defined by the instantaneous coordinates of the slider. The manipulator is also attached to the working platform but is not shown for clarity.

Since range data from any viewpoint are gathered in respect to  $R_{camera}$  while the model is built with respect to  $R_{scene}$  for stability, original measurements  $X_c$  are transformed from  $R_{camera}$  to  $R_{scene}$  as follows:

$$X_s = T_{hs}^{-1} T_{ph}^{-1} T_{pc} X_c \quad (1)$$

where  $T_{hs}$ ,  $T_{ph}$  and  $T_{pc}$  represent the respective homogeneous transformation matrices between the HSTD and the scene, between the platform and the HSTD and between the platform and the range camera.  $X_s$  and  $X_c$  are the range measurements in the scene and in the camera reference frames respectively.

Each component in equation (1) is characterized by some uncertainty which is expressed in terms of a covariance matrix,  $\Lambda$ . Range measurement uncertainty depends on the characteristics of the sensor. Uncertainty on  $T_{ph}$  and  $T_{pc}$  parameters is determined from the precision of calibrating tools used during the platform assembly and the level of precision of the slider controller. The HSTD is another important source of uncertainty in that the spatial relationship  $T_{hs}$  between  $R_{hstd}$  and  $R_{scene}$  is computed

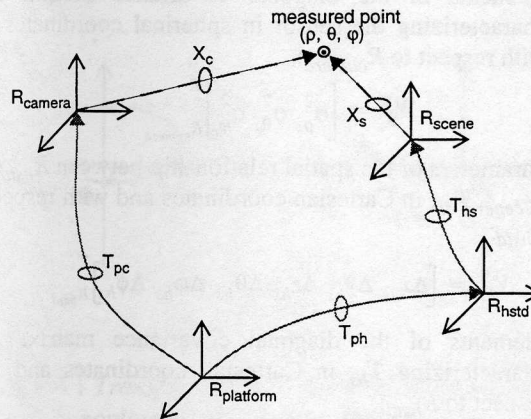


Figure 3 : Uncertain spatial relationships between various reference frames.

within a given range of error. Figure 3 illustrates the respective relationships between each reference frame. The uncertainty is denoted as an ellipse on the corresponding arrow joining two reference frames.

For each range measurement gathered from a given viewpoint, the range sensor provides the coordinates,  $X_c$ , of a point located on an object and the covariance matrix,  $\Lambda_{X_c}$ , of this measurement with respect to  $R_{camera}$ . Simultaneously, the HSTD provides the relative transformation between  $R_{hstd}$  and  $R_{scene}$ ,  $T_{hs}$ , along with the related covariance matrix,  $\Lambda_{hs}$  with respect to  $R_{hstd}$ . The slider controller provides the current parameters of the spatial relationship between  $R_{platform}$  and  $R_{camera}$ ,  $T_{pc}$ , as well as the corresponding covariance matrix,  $\Lambda_{pc}$  with respect to  $R_{platform}$ . Finally, the constant transformation between  $R_{platform}$  and  $R_{hstd}$ ,  $T_{ph}$ , is known by means of calibration along with the related covariance matrix,  $\Lambda_{ph}$  with respect to  $R_{platform}$ .

In order to simplify uncertainty processing, it is assumed that the uncertainty along each axis of a given reference frame is perfectly independent from the uncertainty along the other axes. This results in diagonal covariance matrices. Such a matrix can thus be reduced to a vector,  $W$ , containing the six variance parameters associated to a given covariance matrix,  $\Lambda$ . In a similar manner, spatial relationships are encoded as a set of 6-parameter vectors,  $V$ , containing the 3 translational and the 3 rotational parameters of a given homogeneous transformation in 3-D space.

In other words, for each range measurement from a given viewpoint, the following set of eight vectors is known:

- Spherical coordinates of a point in the scene with respect to  $R_{camera}$ :

$$X_c = \begin{bmatrix} \rho_c & \theta_c & \varphi_c \end{bmatrix}_{R_{camera}}^T \quad (2)$$

- Elements of the diagonal covariance matrix,  $\Lambda_{X_c}$ , characterizing the sensor in spherical coordinates and with respect to  $R_{camera}$ :

$$W_{X_c} = \begin{bmatrix} \sigma_{\rho_c}^2 & & & \\ & \sigma_{\theta_c}^2 & & \\ & & \sigma_{\phi_c}^2 & \\ & & & \end{bmatrix}_{R_{camera}}^T \quad (3)$$

- Parameters of the spatial relationship between  $R_{hstd}$  and  $R_{scene}$ ,  $T_{hs}$ , in Cartesian coordinates and with respect to  $R_{hstd}$ :

$$V_{hs} = \begin{bmatrix} \Delta x_{hs} & \Delta y_{hs} & \Delta z_{hs} & \Delta \theta_{hs} & \Delta \phi_{hs} & \Delta \psi_{hs} \end{bmatrix}_{R_{hstd}}^T \quad (4)$$

- Elements of the diagonal covariance matrix,  $\Lambda_{hs}$ , characterizing  $T_{hs}$  in Cartesian coordinates and with respect to  $R_{hstd}$ :

$$W_{hs} = \begin{bmatrix} \sigma_{\Delta x_{hs}}^2 & & & & & & \\ & \sigma_{\Delta y_{hs}}^2 & & & & & \\ & & \sigma_{\Delta z_{hs}}^2 & & & & \\ & & & \sigma_{\Delta \theta_{hs}}^2 & & & \\ & & & & \sigma_{\Delta \phi_{hs}}^2 & & \\ & & & & & \sigma_{\Delta \psi_{hs}}^2 & \end{bmatrix}_{R_{hstd}}^T \quad (5)$$

- Parameters of the spatial relationship between  $R_{platform}$  and  $R_{hstd}$ ,  $T_{ph}$ , in Cartesian coordinates and with respect to  $R_{platform}$ :

$$V_{ph} = \begin{bmatrix} \Delta x_{ph} & \Delta y_{ph} & \Delta z_{ph} & \Delta \theta_{ph} & \Delta \phi_{ph} & \Delta \psi_{ph} \end{bmatrix}_{R_{platform}}^T \quad (6)$$

- Elements of the diagonal covariance matrix,  $\Lambda_{ph}$ , characterizing  $T_{ph}$  in Cartesian coordinates and with respect to  $R_{platform}$ :

$$W_{ph} = \begin{bmatrix} \sigma_{\Delta x_{ph}}^2 & & & & & & \\ & \sigma_{\Delta y_{ph}}^2 & & & & & \\ & & \sigma_{\Delta z_{ph}}^2 & & & & \\ & & & \sigma_{\Delta \theta_{ph}}^2 & & & \\ & & & & \sigma_{\Delta \phi_{ph}}^2 & & \\ & & & & & \sigma_{\Delta \psi_{ph}}^2 & \end{bmatrix}_{R_{platform}}^T \quad (7)$$

- Parameters of the spatial relationship between  $R_{platform}$  and  $R_{camera}$ ,  $T_{pc}$ , in Cartesian coordinates and with respect to  $R_{platform}$ :

$$V_{pc} = \begin{bmatrix} \Delta x_{pc} & \Delta y_{pc} & \Delta z_{pc} & \Delta \theta_{pc} & \Delta \phi_{pc} & \Delta \psi_{pc} \end{bmatrix}_{R_{platform}}^T \quad (8)$$

- Elements of the diagonal covariance matrix,  $\Lambda_{pc}$ , characterizing  $T_{pc}$  in Cartesian coordinates and with respect to  $R_{platform}$ :

$$W_{pc} = \begin{bmatrix} \sigma_{\Delta x_{pc}}^2 & & & & & & \\ & \sigma_{\Delta y_{pc}}^2 & & & & & \\ & & \sigma_{\Delta z_{pc}}^2 & & & & \\ & & & \sigma_{\Delta \theta_{pc}}^2 & & & \\ & & & & \sigma_{\Delta \phi_{pc}}^2 & & \\ & & & & & \sigma_{\Delta \psi_{pc}}^2 & \end{bmatrix}_{R_{platform}}^T \quad (9)$$

One must note that measurements, spatial relationships and covariance matrices are known in various reference frames while all those data must be merged into one single reference frame attached to the scene. This explains the necessity to propagate the uncertainty among these various reference frames in order to obtain meaningful uncertainty values along each axis of  $R_{scene}$ .

### 3 Uncertainty propagation with Jacobian matrices

Building a rich occupancy model with respect to  $R_{scene}$  implies that range measurements are transformed from  $R_{camera}$  to  $R_{scene}$  by means of equation (1) taking into account the uncertainty on  $X_c$ ,  $T_{hs}$ ,  $T_{ph}$  and  $T_{pc}$ . The uncertainty from each source must be propagated through the transformation chain in order to quantify the corresponding uncertainty with respect to  $R_{scene}$ . Smith et

al. have developed the expressions when two spatial transformations in 3-D space are implied. Here, the development is made for a combination of three spatial relationships in 3 dimensions in accordance with the application described previously.

Measurement coordinates expressed in  $R_{scene}$ ,  $X_s$ , are a nonlinear function,  $f$ , which depends on 21 parameters ( $V_{hs}$ ,  $V_{ph}$ ,  $V_{pc}$  and  $X_c$ ).

$$X_s = f(V_{hs}^{(-1)}, V_{ph}^{(-1)}, V_{pc}, X_c) \quad (10)$$

where  $V_{hs}^{(-1)}$  and  $V_{ph}^{(-1)}$  denote the parameters of the inverse transformations  $T_{hs}^{-1}$  and  $T_{ph}^{-1}$  respectively. This function can be approximated by a linear Taylor series of first order [11], such as:

$$\hat{y} = f(\hat{x}) + J_f \hat{x} \quad (11)$$

where  $J_f$  is the Jacobian matrix of function  $f$  evaluated around the mean value  $\hat{x}$ .

The covariance matrix of measurements in  $R_{scene}$ ,  $\Lambda_{X_s}$ , taking into account all sources of uncertainty is the following:

$$\Lambda_{X_s} = J_f \cdot \Lambda_{W_{hs}^{(-1)}, W_{ph}^{(-1)}, W_{pc}, W_{X_c}} \cdot J_f^T \quad (12)$$

[3x3] [3x21] [21x21] [21x3]

where  $\Lambda_{W_{hs}^{(-1)}, W_{ph}^{(-1)}, W_{pc}, W_{X_c}}$  is a covariance matrix composed of four submatrices containing respectively  $W_{hs}^{(-1)}$ ,  $W_{ph}^{(-1)}$ ,  $W_{pc}$  and  $W_{X_c}$  on their diagonal. Since each transformation as well as each measurement are independent of each other, the global covariance matrix is also diagonal.

Equation (12) can be developed as follows:

$$\Lambda_{X_s} = J_{f_{V_{hs}^{(-1)}}} \Lambda_{W_{hs}^{(-1)}} J_{f_{V_{hs}^{(-1)}}}^T + J_{f_{V_{ph}^{(-1)}}} \Lambda_{W_{ph}^{(-1)}} J_{f_{V_{ph}^{(-1)}}}^T + J_{f_{V_{pc}}} \Lambda_{W_{pc}} J_{f_{V_{pc}}}^T + J_{f_{X_c}} \Lambda_{W_{X_c}} J_{f_{X_c}}^T \quad (13)$$

but special attention must be paid to the covariance matrices of inverse transformations,  $\Lambda_{W_{hs}^{(-1)}}$  and  $\Lambda_{W_{ph}^{(-1)}}$ . Considering a general inverse transformation such that:

$$X = T_{\alpha}^{-1} \cdot X \quad (14)$$

The corresponding covariance matrix is obtained as follows [12]:

$$\Lambda_{W_{\alpha}^{(-1)}} = J_{V_{\alpha}^{(-1)}} \Lambda_{W_{\alpha}} J_{V_{\alpha}^{(-1)}}^T \quad (15)$$

where:

$$J_{V_{\alpha}^{(-1)}} = \frac{\delta X}{\delta \bar{X}} \quad (16)$$

Equation (13) is finally expressed as follows for a composition of two inverse spatial transformations and one direct transformation in order to evaluate the covariance matrix resulting from the propagation of four sources of uncertainty towards a single reference frame, for instance  $R_{scene}$ .

$$\begin{aligned} \Lambda_{X_s} = & J_{f_{V_{hs}^{(-1)}}} \cdot J_{V_{hs\emptyset}^{(-1)}} \cdot \Lambda_{W_{hs}} \cdot J_{V_{hs\emptyset}^{(-1)}}^T \cdot J_{f_{V_{hs}^{(-1)}}}^T \\ & + J_{f_{V_{ph}^{(-1)}}} \cdot J_{V_{ph\emptyset}^{(-1)}} \cdot \Lambda_{W_{ph}} \cdot J_{V_{ph\emptyset}^{(-1)}}^T \cdot J_{f_{V_{ph}^{(-1)}}}^T \\ & + J_{f_{V_{pc}}} \cdot \Lambda_{W_{pc}} \cdot J_{f_{V_{pc}}}^T + J_{f_{X_c}} \cdot \Lambda_{W_{X_c}} \cdot J_{f_{X_c}}^T \end{aligned} \quad (17)$$

Applying equations (1) and (17) to each range measurement with respect to  $R_{camera}$ ,  $X_c$ , provides the corresponding coordinates with respect to  $R_{scene}$ ,  $X_s$ , as well as the related uncertainty on  $X_s$  taking into account every sources of error in the system.

This constitutes a very rigorous approach for the estimation of uncertainty in the scene reference frame. But the complexity of the estimation of the covariance matrix,  $\Lambda_{X_s}$ , depends on the number of chained transformations and on the fact that some of these relationships are inverted such as  $T_{hs}^{-1}$  and  $T_{ph}^{-1}$  in the considered application. The resulting closed-form expressions of equations (1) and (17) are relatively complex and the required evaluation of each Jacobian matrix for each measurement is computationally intensive. The overhead added to the model building algorithm is therefore significant. An alternative approach which avoids the use of Jacobian matrices is presented in section 4.

#### 4 Probabilistic uncertainty propagation through reference frame relationships

Julier and Uhlmann [5] have proposed a strategy to propagate uncertainty across nonlinear relationships such as spatial transformations between two reference frames. The approach consists in applying the nonlinear relationship to a probabilistic distribution centered on the measured point in the first reference frame whose dimensions are augmented to match the total number of degrees of freedom implied in the nonlinear relationship and in the measurement. The initial probabilistic distribution is characterized by the variance along each axis of the augmented reference frame,  $R_1$ . Applying the nonlinear relationship to this distribution results in a new probabilistic distribution defined with respect to the axes of the second reference frame,  $R_2$ , as shown in figure 4. Estimating the mean and the covariance along each axis of the new distribution provides the measurement coordinates and the uncertainty values relative to the second reference frame.

In the particular application of interest, the nonlinear relationship depends on 21 parameters as defined in section

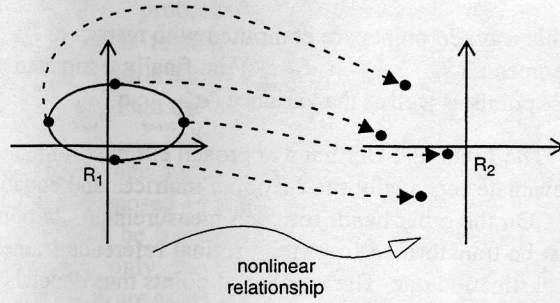


**Figure 4 :** Transformation of a probabilistic distribution across a nonlinear relationship between two reference frames as proposed by Julier and Uhlmann.

3. The initial reference frame considered is  $R_{camera}$  augmented to 21 dimensions. The nonlinear relationship provides a second probabilistic distribution with respect to  $R_{scene}$  which is also augmented to 21 dimensions. But since we are only interested in the coordinates and the uncertainty of measurements along the  $x$ ,  $y$  and  $z$  axes of  $R_{scene}$ , only these three parameters are considered thus reducing the computational complexity.

Nevertheless, in accordance to Julier and Uhlmann, the probabilistic distribution in the initial reference frame must be defined as a set of  $2n$  points for a  $n$ -dimensional system (here  $n = 21$ ). This is the minimal set of data required in order to preserve the probabilistic distribution moments in both reference frames. Therefore, for each measurement, the nonlinear relationship must be applied to  $2n$  points in order to estimate their coordinates with respect to  $R_{scene}$  by computing the mean and the variance along the  $n$  axes (only three in this application).

The approach starts with the global covariance matrix,  $\Lambda_{W_{hs}^{(-1)}, W_{ph}^{(-1)}, W_{pc}, W_{X_c}}$  previously defined. The first step consists in extracting the square root of  $n \cdot \Lambda_{W_{hs}^{(-1)}, W_{ph}^{(-1)}, W_{pc}, W_{X_c}}$  in order to estimate the standard deviations along each axis. The Cholesky method [10] is well suited for this task. The  $2n$  points,  $pt[i]$ , included in the probabilistic distribution sample are defined as each column which compose the two matrices resulting from the square root extraction  $\pm \sqrt{n \cdot \Lambda_{W_{hs}^{(-1)}, W_{ph}^{(-1)}, W_{pc}, W_{X_c}}}$ . The mean value of each parameter is added to these coordinates in order to center the sample on the real data values.

The nonlinear relationship of equation (10) is applied to the  $2n$  points contained in the sample but only the three first dependent parameter means and covariances are evaluated such that:

$$x_{R_{scene}} [i] = f_1 (pt [i]) \quad (18)$$

$$y_{R_{scene}} [i] = f_2 (pt [i]) \quad (19)$$

$$z_{R_{scene}} [i] = f_3(p_t [i]) \quad (20)$$

In this way,  $2n$  points are computed with respect to  $R_{scene}$ . The mean  $(\hat{x}_{R_{scene}}, \hat{y}_{R_{scene}}, \hat{z}_{R_{scene}})$  is finally estimated on these points as well as the variance  $(\sigma_{x_{R_{scene}}}^2, \sigma_{y_{R_{scene}}}^2, \sigma_{z_{R_{scene}}}^2)$ .

The Julier and Uhlmann approach eliminates the need to evaluate repeatedly the Jacobian matrices and equation (17). On the other hand, for each measurement,  $2n$  points must be transformed from the original reference frame to the destination one. The number of points thus depends on the number of degrees of freedom implied in the nonlinear relationship.

## 5 Applying uncertainty propagation to probabilistic octree model building

In order to merge the knowledge about the uncertainty into the probabilistic octree models, the uncertainty propagation must be adapted to multiple local occupancy grid merging. Elfes [1, 2] uses a blurring convolution process to take into account the uncertainty on a mobile robot position with respect to the global occupancy map. Such an approach could be used in 3-D space. It would result in convoluting a 3-D spherical mask with each local occupancy grid as shown in figure 5 before merging those grids together as described in [8]. But this strategy has an important limitation. Since only the first three terms of the nonlinear relationship are computed (eqs. (18), (19), (20)), only the uncertainty on the local grid position is considered with respect to  $R_{scene}$  while the uncertainty on the orientation of  $R_{camera}$  is neglected. This could lead to significant errors on the uncertainty estimation relative to  $R_{scene}$  and therefore limits the suitability of merging this supplementary information into the model.

An adaptation of the closed-form OPD computation is proposed that allows taking into account both the uncertainty on position and orientation originating from all sources. The technique consists in transforming each measurement from  $R_{camera}$  to  $R_{scene}$  taking advantage of the Julier and Uhlmann approach. This results in a distribution of measurement points referred to  $R_{scene}$

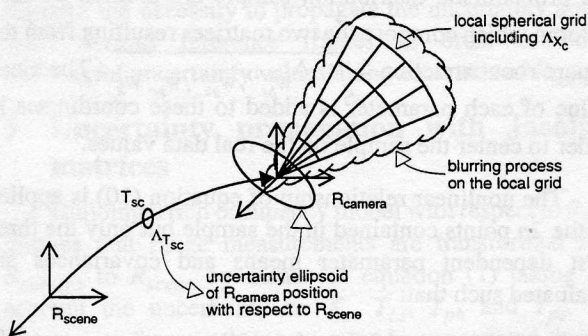


Figure 5 : Blurring process on a local spherical occupancy grid in order to consider the uncertainty.

$(X_{R_{scene}}, \Lambda_{R_{scene}})$  which depends both on the position and on the orientation uncertainties. In term of the closed-form OPD approximation, this provides knowledge about the uncertainty of the sensor position, which corresponds to the origin of the corresponding local spherical occupancy grid as shown in figure 6. Ellipses represent the uncertainty on measurements and on the origin of the area scanned by the sensor. The initial closed-form OPD approximation is thus extended behind the sensor as shown in figure 7. It is known that between the sensor and the object surface, the occupancy probability is 0 since there is only empty space. Nearby the object, the probability grows in a Gaussian-like manner and drops to 0.5 (*unknown*) behind the object since the sensor cannot scan the area that is hidden by the object. A similar behavior is expected around the sensor position. Behind the sensor, the state of the space remains unknown ( $p = 0.5$ ). Since the sensor position is not perfectly known because of the uncertainty on the transformation chain, the step between unknown area (behind the sensor) and empty space (in front of the sensor) is not accurately located. For this reason, the occupancy probability near the origin of  $R_{camera}$  drops down in a Gaussian-like manner from 0.5 to 0.0. Figure 7 shows the new closed-form OPD approximation for a 1-D space. In practice, the probabilistic distribution is used in 3-D space.

To avoid building huge local spherical occupancy grids which would result in a heavy computational load if the closed-form OPD approximation was centered on  $R_{scene}$ , the OPD is computed on a parametric straight line,  $\vec{d}_i$ , which corresponds to the laser beam axis while data is

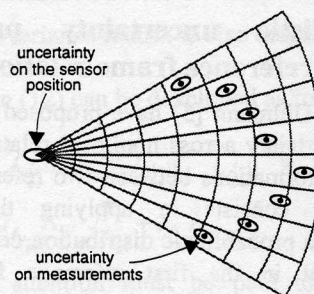


Figure 6 : Uncertainty ellipses around the sensor position and the measurements.

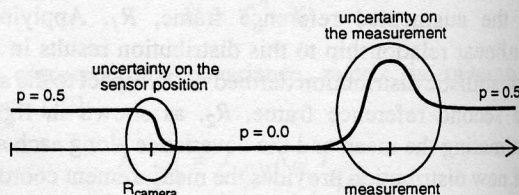
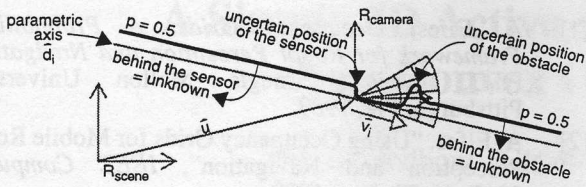


Figure 7 : Extended closed-form occupancy probability distribution approximation for a 1-D space with uncertainty on sensor position and on range measurements.



**Figure 8 :** Parametric closed-form OPD approximation for a measurement point estimated with respect to  $R_{scene}$  gathered as shown in figure 8 for 2-D space.

$$\hat{d}_i = \hat{u} + \lambda \hat{v}_i \quad (21)$$

This allows the processing of the measurements transformed with respect to  $R_{scene}$  with the extended closed-form OPD approximation. Both the uncertainties on range measurements and on the sensor position are included into the local spherical grid which results from the application of the parametric OPD with respect to  $R_{scene}$ . Considering that measurements from a given viewpoint are gathered in a short period of time compared to perturbations, the origin of the local spherical grid is assumed to be constant. This condition must be satisfied in order to ensure the validity of the approach. This also ensures that the original range data merging strategy of local spherical grids can be applied to build the global Cartesian model.

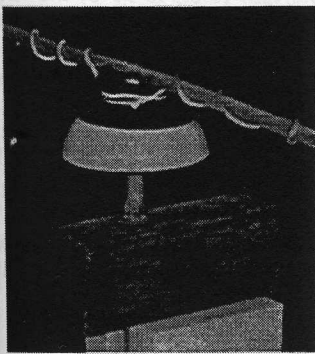
Nevertheless, the OPD parametric straight line must be evaluated for each measurement since the laser beam has a different orientation for each point while always crossing the same origin. This allows considering non uniform uncertainty distributions which characterize most range sensors [7].

This approach is promising since it allows the integration of uncertainty from the sensor and from the transformation chain into the model without having to evaluate the complex expression of Jacobian matrices, eq. (17), for each measurement. Moreover, since transformed

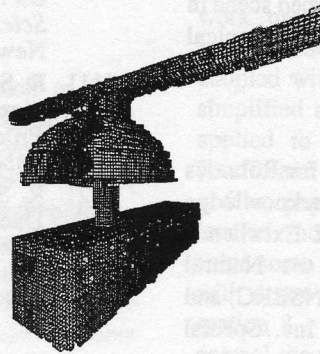
measurements relative to  $R_{scene}$  are used to estimate the occupancy probability distribution, rather than measurements relative to  $R_{camera}$  as in Elfes' approach, both the position and the orientation uncertainties are taken into account. On the other hand, the nonlinear relationship between  $R_{camera}$  and  $R_{scene}$  must be evaluated for  $2n$  points for each range measurement. When the data gathering strategy proposed in section 2 is used, this means that 42 points must be transformed for each range measurement. But since only the three first terms of the nonlinear relationship are of interest and since processing these terms is limited to a matrix product, this appears to be less computationally intensive than the evaluation of Jacobian matrices.

## 6 Necessity of uncertainty integration

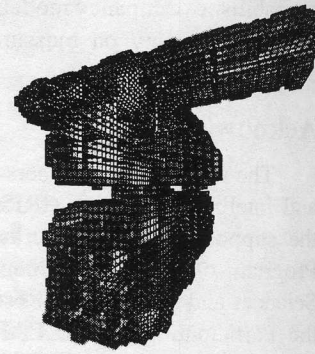
Because of the large number of points to be transformed from  $R_{camera}$  to  $R_{scene}$ , the necessity to integrate knowledge about the uncertainty in an occupancy model must be considered with care. The computational overhead required for processing this supplementary data is not justified for all applications. Nevertheless, in the context of on-line electricity distribution equipment maintenance, neglecting the uncertainty on measurements could result in dangerous operations threatening both the operator, the telemanipulator and the stability of the electricity network. Security considerations are then of prime importance and the model reliability is essential. Figure 9 shows the impact of uncertainty on the extent of a modeled electrical insulator holding a wire as shown in (a). Gray shading of the octree cells corresponds to their respective occupancy probability; white being 100% (*occupied*) and black 0% (*empty*). No uncertainty is taken into account in building the model in (b). This case corresponds to gathering range measurements with an ideal sensor on a perfectly stable object. When an uncertainty of 10 mm in position and 0.5 degree in orientation is considered as in (c), the resulting model is blurred and therefore the model components are larger than in (b). A lower occupancy probability is also found at the object



(a)



(b)



(c)

**Figure 9 :** Occupancy model of an electrical wire attached to an insulator mounted on a beam: (a) the real setup, (b) the model when an ideal data gathering system is used (no uncertainty), (c) the model when uncertainty is quantified.

surfaces since the separation between occupied and free space is not perfectly defined. In a collision-free path planning application, a wider occupied region must be considered in order to avoid any contact between the robot and the objects. If the uncertainty is neglected or underestimated, a model such as (b) could be obtained even though parts of the objects lie outside the area tagged as occupied. Adding the uncertainty knowledge provides models that lead to safer path planning.

However, an overestimation of the uncertainty will lead to obstacles which appear significantly wider than they actually are. Free space between obstacles can then be considerably reduced. Such a model would be prejudicial to efficient operation. A compromise must then be realized between the requested supplementary computing time, the model reliability and the necessary security level. This solely depends on the application in which the model is intended to serve and on the available processors.

## 7 Concluding remarks

In this paper, a strategy to merge an estimate of the uncertainty on the occupancy probability into an octree model of cluttered workspace has been presented. A range data gathering scheme taking into account the external perturbations on an outdoor scene has been proposed. This scheme implies a 3-step spatial transformation chain to transpose range data from the camera reference frame to the model reference frame attached to the scene. A rigorous uncertainty propagation approach using Jacobian matrices has been developed and was shown to lead to an important computational load. The Julier and Uhlmann probabilistic distribution propagation scheme through nonlinear transformations has appeared to be more suitable for the probabilistic occupancy model building algorithm. Its capacity to take into account the uncertainty on both the position and the orientation without complex matrix derivation and evaluation is an important advantage. Finally, an adaptation of the closed-form approximation of the occupancy probability distribution function proposed in a previous paper has been presented. It allows to build probabilistic occupancy models of a 3-D perturbed scene in which uncertainty on measurements and on mechanical calibration is integrated.

## Acknowledgments

The authors are members of the Institute for Robotics and Intelligent Systems (IRIS) and wish to acknowledge the support of the Networks of Centres of Excellence Program of the Government of Canada, the Natural Sciences and Engineering Research Council (NSERC) and the Participation of PRECARN Associates Inc. Special thanks are also addressed to Dr Patrick Hébert whose comments were greatly appreciated in the initial development of this approach.

## References

- [1] A. Elfes, *Occupancy Grids: A Probabilistic Framework for Robot Perception and Navigation*, Ph.D. thesis, Carnegie Mellon University, Pittsburgh, PA, 1989.
- [2] A. Elfes, "Using Occupancy Grids for Mobile Robot Perception and Navigation", *IEEE Computer*, 22(6):46-57, June 1989.
- [3] P. Hébert, S. Betgé-Brezetz and R. Chatila, "Probabilistic Map Learning: Necessity and Difficulties", in *Proceedings of the International Workshop on Reasoning with Uncertainty in Robotics*, Amsterdam, The Netherlands, December 4-6, 1995.
- [4] L. D. Hostetler and R. D. Andreas, "Nonlinear Kalman Filtering Techniques for Terrain-Aided Navigation", in *IEEE Transactions on Automation and Control*, vol. AC-28, pp. 315-323, March 1983.
- [5] S. Julier and J. Uhlmann, *A General Method for Approximating Nonlinear Transformations of Probability Distributions*, Technical Report, Robotics Research Group, Oxford University, UK, 1994.
- [6] T. Kanade, A. Yoshida, K. Oda, H. Kano and M. Tanaka, "A Stereo Machine for Video-Rate Dense Depth Mapping and its New Applications", in *Proceedings of the IEEE 15th Computer Vision and Pattern Recognition Conference*, San Francisco, CA, 1996.
- [7] F. Loranger, *Fusion Multisensorielle pour la Modélisation de l'Espace de Travail d'un Véhicule Autopiloté*, Technical Report, Computer Vision and Digital Systems Laboratory, Laval University, Québec, Canada, August 1994.
- [8] P. Payeur, P. Hébert, D. Laurendeau and C. M. Gosselin, "Probabilistic Octree Modeling of a 3-D Dynamic Environment", in *Proceedings of the IEEE International Conference on Robotics and Automation*, pp. 1289-1296, Albuquerque, NM, April 1997.
- [9] P. Payeur, D. Laurendeau, C. M. Gosselin, "Range Data Merging for Probabilistic Octree Modeling of 3-D Workspaces", in *Proceedings of the IEEE International Conference on Robotics and Automation*, Leuven, Belgium, May 1998.
- [10] W. H. Press, S. A. Teukolsky, W.T. Vetterling and B.P. Flannery, *Numerical Recipes in C, the Art of Scientific Computing*, Cambridge University Press, New York, 2nd edition, 1992.
- [11] R. Smith, M. Self and P. Cheeseman, "A Stochastic Map for Uncertain Spatial Relationships", in *Proceedings of the 4th International Symposium on Robotics Research*, MIT Press, pp. 467-474, 1988.
- [12] R. Smith, M. Self and P. Cheeseman, "Estimating Uncertain Spatial Relationships in Robotics", in I.J. Cox and G.T. Wilfong, editors, *Autonomous Robot Vehicles*, Springer-Verlag, New York, pp. 167-193, 1990.